Joint migration velocity analysis of PP- and PS-waves for VTI media

Pengfei Cai & Ilya Tsvankin
Center for Wave Phenomena, Colorado School of Mines

ABSTRACT
Combining PP-waves with mode-converted PS-waves in migration velocity analysis (MVA) can help build more accurate VTI (transversely isotropic with a vertical symmetry axis) velocity models. To take advantage of efficient MVA algorithms designed for pure modes, here we generate pure SS-reflections from PP and PS data using the PP+PS=SS method. Then the residual moveout in both PP and SS common-image gathers is minimized during iterative velocity updates. The model is divided into square cells, and the VTI parameters V_{P0}, V_{S0}, ϵ, and δ are defined at each grid point. The objective function also includes the differences between the migrated depths of the same reflectors on the PP and SS sections. The replacement of PS-waves with pure SS reflections in MVA allows us to avoid problems caused by the moveout asymmetry and other undesirable features of mode conversions. Synthetic examples confirm that 2D MVA of PP- and PS-waves can resolve all four relevant parameters of VTI media if reflectors with at least two distinct dips are available. After the velocity model has been reconstructed, accurate depth images can be obtained by migrating the recorded PP and PS data.

Key words: joint migration velocity analysis, PS-waves, VTI, codepthing

1 INTRODUCTION

Prestack depth migration (PSDM) and reflection tomography in the migrated domain are widely used in P-wave imaging (Stork, 1992; Wang et al., 1995; Adler et al., 2008; Bakulin et al., 2010). Most current PSDM and migration velocity analysis (MVA) algorithms account for transverse isotropy with a vertical (VTI) or tilted (TTI) symmetry axis. Sarkar and Tsvankin (2004) develop an efficient MVA method for VTI media by dividing the model into factorized blocks. Within each block, the anisotropy parameters are constant, while the P-wave symmetry-direction velocity V_{P0} varies linearly in space. To extend MVA to more complex subsurface structures, Wang and Tsvankin (2010) suggest a P-wave ray-based gridded tomographic algorithm in which the parameters V_{P0}, ϵ, and δ are defined on a rectangular grid. Similar multiparameter tomographic inversion is applied to synthetic and field P-wave data by Zhou et al. (2011).

To resolve the velocity V_{P0} and anisotropy parameters ϵ and δ required for P-wave depth imaging, it is necessary to combine P-wave traveltimes with additional information. Tsvankin and Thomsen (1995) demonstrate that long-spread (nonhyperbolic) P- and SV-wave moveouts are sufficient for estimating the VTI parameters V_{P0}, ϵ, δ, and the SV-wave vertical velocity V_{S0}. However, it is more practical to supplement P-waves with converted PS(PSV) data. For 2D VTI models, the parameters V_{P0}, V_{S0}, ϵ, and δ can be obtained by combining PP- and PS-wave traveltimes for a horizontal and dipping interface (Tsvankin and Grechka, 2000).

Several authors discuss joint tomographic inversion of PP and PS data (Stopin and Ehinger, 2001; Audebert et al., 1999; Broto et al., 2003; Foss et al., 2005). However, velocity analysis of mode convertions is hampered by the asymmetry of PS moveout (i.e. PS traveltimes generally do not stay the same when the source and receiver are interchanged) and polarity reversals of PS-waves. As discussed by Thomsen (1999) and Tsvankin and Grechka (2011), the apex of the PS moveout in common-midpoint (CMP) gathers typically is shifted from zero offset. Therefore, MVA for PS-waves (Du et al., 2012; Foss et al., 2005; Audebert et al., 1999) has to account for the "diodic" nature of PS reflections (Thomsen, 1999). For example, common-image gathers (CIGs) of PS-waves can be computed separately for positive and negative offsets in the tomographic objective function (Foss et al., 2005).

To replace mode conversions in velocity analysis with pure SS reflections, Grechka and Tsvankin (2002) suggest the so-called PP+PS=SS method. By combining PP and PS events that share P-legs, that method generates SS reflection data with the correct kinematics. Grechka et al. (2002b) perform joint inversion of PP and PS reflection data using so-called

stacking-velocity tomography, which operates with NMO velocities for 2D lines and NMO ellipses for wide-azimuth 3D surveys (Grechka et al., 2002a). They construct SS traveltimes with the PP+PS=SS method and then apply stacking-velocity tomography to the PP and SS data. However, their methodology is limited to hyperbolic moveout and excludes information contained in long-offset traveltimes (Tsvankin and Grechka, 2011). Also, stacking-velocity tomography can be applied only to relatively simple layered or blocked models.

To make use of the efficient MVA techniques developed for pure modes (Sarkar and Tsvankin, 2004; Wang and Tsvankin, 2010), here we apply the PP+PS=SS method to construct pure SS-wave reflections from PP and PS data. The MVA is performed by minimizing residual moveout of reflection events in both PP- and SS-wave CIGs. Our velocity-updating for P-wave data is based on the ray-based gridded tomography developed by Wang and Tsvankin (2010). PP and PS images of the same reflector do not match in depth if the velocity model is incorrect (Foss et al., 2005; Tsvankin and Grechka, 2011). Therefore, in addition to flattening image gathers, we penalize depth misties between PP and PS sections.

First, we introduce the methodology of joint MVA of PP- and PS-waves, which includes identification (registration) of PP and PS events from the same interface, application of the PP+PS=SS method to create SS reflection data, and joint MVA of the recorded PP- and generated SS-waves. Next, we test the algorithm on a simple model comprised of a VTI layer sandwiched between isotropic media and on a layered model that includes a dipping reflector (e.g., a fault plane). The testing shows that for the second model the joint MVA algorithm can resolve the VTI parameters without additional information.

2 METHODOLOGY

P-wave reflection traveltimes generally are insufficient to resolve the parameters V_{P0}, ϵ, and δ required for P-wave depth imaging in VTI media. Therefore, to build a VTI model for prestack depth migration, at least one medium parameter (e.g., V_{P0}) must be known a priori (Sarkar and Tsvankin, 2004).

As discussed in Tsvankin and Grechka (2000), combining P-wave traveltimes with the moveout of PS-waves converted at a horizontal and dipping interface can help constrain the vertical P- and SV-wave velocities and the parameters ϵ and δ. The most significant problem in PS-wave velocity analysis is the moveout asymmetry with respect to zero offset in CMP geometry (Tsvankin and Grechka, 2011). Unless the model is laterally homogeneous and has a horizontal symmetry plane, the PS traveltime does not stay the same when the source and receiver are interchanged. Therefore, most migration velocity analysis methods designed for pure modes cannot be directly applied to converted waves. Here, we employ the PP+PS=SS method (Grechka and Tsvankin, 2002) to produce pure SS reflection events from the PP and PS reflections generated at the same interface.

Implementation of the PP+PS=SS method requires event registration, or identification of PP and PS reflections from the same interfaces. The main idea of the method is to combine PP and PS events that share the same P-legs. This is done by matching time slopes (horizontal slownesses) on common-receiver gathers of PP- and PS-waves (Figure 1). Then the traveltime of the constructed SS wave (sometimes called the "pseudo-S" arrival) is given by:

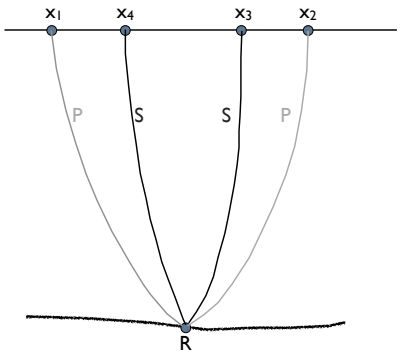

Figure 1. Matching the horizontal slownesses on common-receiver PP and PS sections at locations x_1 and x_2 helps find the source-receiver coordinates x_3 and x_4 of the pure SS ray x_3Rx_4. This reconstructed SS ray has the same reflection point R as the PP ray x_1Rx_2 and PS rays x_1Rx_3 and x_2Rx_4 (after Grechka and Tsvankin, 2002).

$$t_{SS}(x_3, x_4) = t_{PS}(x_1, x_3) + t_{PS}(x_2, x_4) - t_{PP}(x_1, x_2). \tag{1}$$

While the constructed SS-wave traveltimes are exact, the PP+PS=SS cannot produce correct reflection amplitudes. Hence, we convolve the SS traveltimes with a Ricker wavelet to generate "pseudo" SS reflection data to be used for MVA. The maximum reflection angle of the shear wave generated by mode conversion in a horizontal isotropic layer with the P- and S-wave velocities V_P and V_S is $\theta_S^{\rm crit} = \sin^{-1}(V_S/V_P)$, and the half-offset h_S cannot exceed the critical value,

$$h_S^{\rm crit} = D\, \tan\left[\sin^{-1}\left(\frac{V_S}{V_P}\right)\right]; \tag{2}$$

D is the layer's thickness. For example, for a typical $V_S/V_P = 1/2$, the maximum half-offset is less than 0.6D. Therefore, it is necessary to include long-offset PP and PS data to generate SS data suitable for robust velocity analysis. The offsets of the computed SS-wave are smaller than those for the acquired PP and PS data but may be sufficient for MVA if the survey includes offsets reaching two target depths.

Here, we extend the MVA algorithm of Wang and Tsvankin (2010) to multicomponent (PP and SS) data. The model is divided into square cells, and the parameters V_{P0}, V_{S0}, ϵ, and δ are defined at each grid point. We apply prestack Kirchhoff depth migration to both PP and SS data starting with initial isotropic velocity models. The moveouts of migrated PP and SS events in common-image gathers serve as input to the joint MVA. To constrain the parameters η and ϵ, the moveout in PP CIGs is described by the nonhyperbolic equation (Sarkar

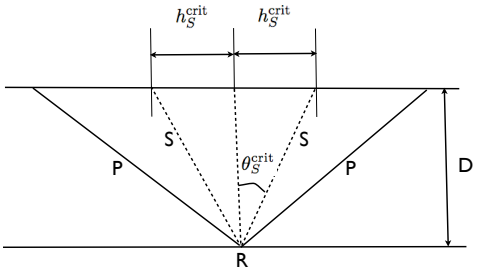

Figure 2. Critical (Maximum) offset of the constructed SS-waves in a horizontal layer (Tsvankin and Grechka, 2011).

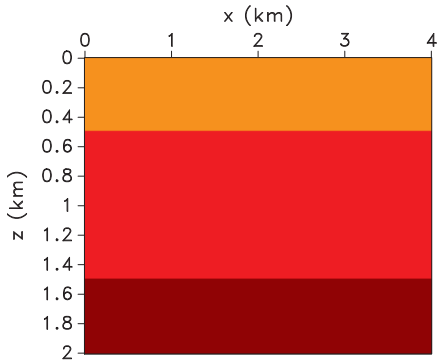

Figure 3. Model with a VTI layer embedded between two isotropic layers. The parameters of the top layer are $V_P = 2000$ m/s, $V_S = 1000$ m/s; for the second layer, $V_{P0} = 3000$ m/s, $V_{S0} = 1500$ m/s, $\epsilon = 0.1$, and $\delta = -0.1$.

and Tsvankin, 2004):

$$z^2(h) = z^2(0) + Ah^2 + B\frac{h^4}{h^2 + z^2(0)}, \qquad (3)$$

where z is the migrated depth, and the coefficients A and B are found by a 2D semblance scan. There is no need to apply equation 3 to SS-wave CIGs because the offset-to-depth ratio of the constructed SS events seldom exceeds 1-1.2. For the joint MVA, we not only minimize the residual moveout in PP and SS CIGs, but also perform codepthing, which involves tying PP and SS images of the same reflectors. The objective function includes a term that penalizes the mismatch in depth of PP and SS migrated images using a selection of key reflection points. Those points are chosen on the basis of coherency and focusing (Foss et al., 2005).

To update model parameters, it is necessary to compute traveltime derivatives with respect to the model parameters (Wang and Tsvankin, 2010). Since we operate with PP- and SS-waves, the parameter set includes not just $V_{\rm P0}$, ϵ, and δ, but also the shear-wave vertical velocity $V_{\rm S0}$. The exact P- and SV-wave phase velocities in VTI media can be expressed as (Tsvankin, 2005):

$$\begin{aligned}\frac{V^2}{V_{\rm P0}^2} &= 1 + \epsilon\sin^2\theta - \frac{f}{2} \\ &\pm \frac{f}{2}\sqrt{1 + \frac{4\sin^2\theta}{f}(2\delta\cos^2\theta - \epsilon\cos 2\theta) + \frac{4\epsilon^2\sin^4\theta}{f^2}}, \end{aligned} \qquad (4)$$

where θ is the phase angle with the symmetry axis and $f \equiv 1 - \frac{V_{\rm S0}^2}{V_{\rm P0}^2}$. The plus in front of the radical corresponds to P-waves and minus to S-waves. For purposes of MVA, however, it is convenient to replace ϵ and δ with the P-wave horizontal ($V_{\rm hor,P}$) and NMO ($V_{\rm nmo,P}$) velocities given by $V_{\rm hor,P} = V_{P0}\sqrt{1+2\epsilon}$ and $V_{\rm nmo,P} = V_{P0}\sqrt{1+2\delta}$. We compute the traveltime derivatives with respect to $V_{\rm hor,P}$ and $V_{\rm nmo,P}$ instead of ϵ and δ. The MVA algorithm updates V_{P0}, V_{S0}, $V_{\rm hor,P}$, and $V_{\rm nmo,P}$ and then converts $V_{\rm hor,P}$ and $V_{\rm nmo,P}$ to ϵ and δ.

The objective function used in the joint MVA is as follows:

$$\begin{aligned} F(\mathbf{\Delta}\lambda) &= \mu_1||\mathbf{A}_P\,\mathbf{\Delta}\lambda + \mathbf{b}_P||^2 + \mu_2||\mathbf{A}_S\,\mathbf{\Delta}\lambda + \mathbf{b}_S||^2 \\ &+ \mu_3||\mathbf{D}\,\mathbf{\Delta}\lambda + \mathbf{y}||^2 + \zeta||L\,\mathbf{\Delta}\lambda||^2, \end{aligned} \qquad (5)$$

where $\mathbf{A}_P$ and $\mathbf{A}_S$ depend on the derivatives of the PP and SS migrated depths with respect to the medium parameters, the vectors $\mathbf{b}_P$ and $\mathbf{b}_S$ contain elements that characterize the residual moveout in PP- and SS-wave CIGs, the matrix $\mathbf{D}$ describes the differences between the derivatives of the PP and SS migrated depths with respect to the medium parameters, and the vector $\mathbf{y}$ contains the differences between the migrated depths on the PP and SS sections. The full definitions of $\mathbf{A}_P$, $\mathbf{A}_S$, $\mathbf{D}$, $\mathbf{b}_P$, $\mathbf{b}_S$, and $\mathbf{y}$ are given in Appendix A. Minimizing the first two terms ($||\mathbf{A}_P\mathbf{\Delta}\lambda + \mathbf{b}_P||^2$ and $||\mathbf{A}_S\mathbf{\Delta}\lambda + \mathbf{b}_S||^2$) allows us to flatten PP and SS CIGs. Codepthing is achieved through minimizing the third term ($||\mathbf{D}\mathbf{\Delta}\lambda + \mathbf{y}||^2$). Because the tomographic inversion can be ill-posed, we add a regularization term ($||L\mathbf{\Delta}\lambda||$) to the objective function. The coefficients μ_1, μ_2, μ_3 and ζ govern the weights of the corresponding terms. The objective function is minimized by a least-squares algorithm.

3 TESTS ON SYNTHETIC DATA

We use anisotropic ray-tracing package ANRAY to generate PP- and PS-wave reflection traveltimes for synthetic tests. ANRAY is developed by the consortim project "Seismic Waves in Complex 3D Structures" (SW3D) at Charles University in Prague. PP and SS images are generated with Kirchhoff prestack depth migration (Seismic Unix program 'sukdmig2d'). To create traveltime tables of PP- and SS-waves, we perform ray tracing using SU code 'rayt2dan'.

We first test the algorithm on a simple horizontally layered model (Figure 3) that includes a VTI layer sandwiched between isotropic media. Without dipping interfaces, the interval parameters for this model cannot be constrained by PP and PS reflection traveltimes. Therefore, the P-wave vertical

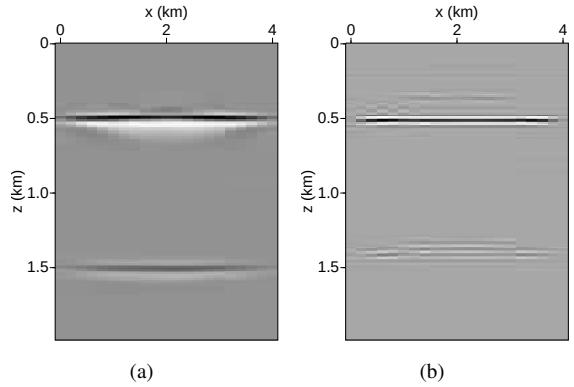

Figure 4. (a) PP-wave and (b) SS-wave depth images computed with the initial model parameters.

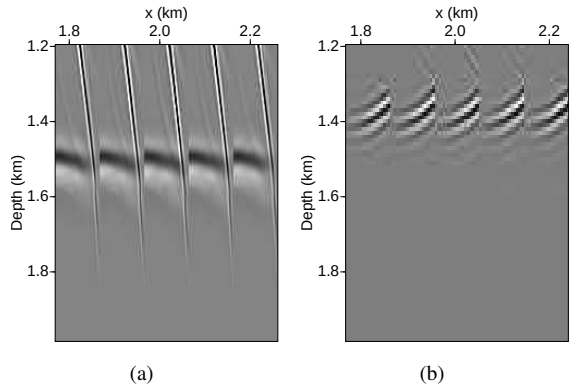

Figure 5. Common-image gathers of (a) PP-waves and (b) SS-waves (displayed every 100 m) after migration with the initial model.

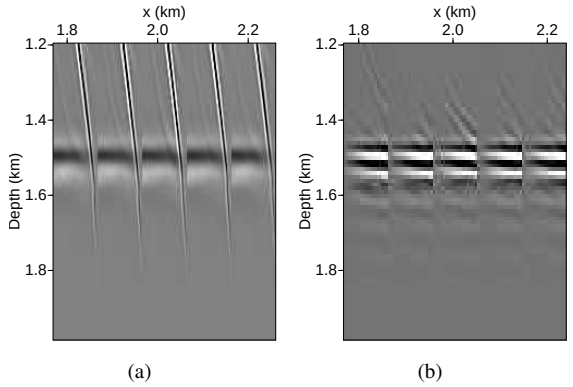

Figure 6. CIGs of (a) PP-waves and (b) SS-waves after migration with the inverted model.

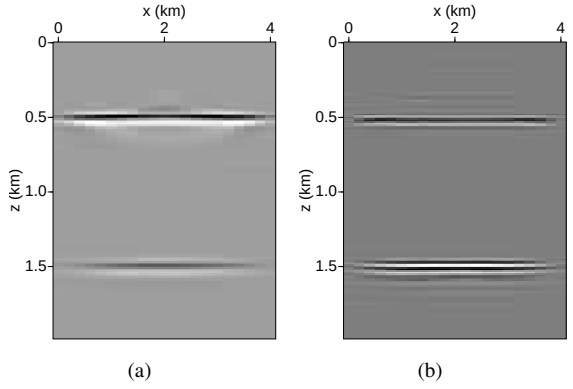

Figure 7. Final depth images of (a) PP-waves and (b) SS-waves with the inverted model parameters.

velocity V_{P0} is assumed to be known, and we invert only for V_{S0} and the anisotropy parameters ϵ and δ of the VTI layer.

The top layer is known to be isotropic and its P- and S-wave velocities can be easily computed from reflection data. The initial S-wave vertical velocity for the middle layer has an error of 10%, and both ϵ and δ are set to zero. The maximum offset-to-depth ratio for the bottom of the VTI layer is close to two, which is sufficient for applying the PP+PS=SS method. Indeed, the maximum offset for recorded PP data is 3 km and the maximum offset for constructed SS data is 1.6 km. The whole PP data set is used along with the SS-waves to estimate the residual moveout in CIGs. For codepthing, however, we only use conventional-spread PP data with offsets not exceeding those for SS-waves.

Figures 4(a) and 4(b) show the PP- and SS-wave migrated sections obtained with the initial model. The bottom of the VTI layer is poorly focused and is imaged at different depths on the PP and SS sections; also, the PP and SS image gathers are not flat (Figures 5(a) and 5(b)).

CIGs used for velocity analysis are uniformly sampled from 1 to 3 km along the second reflector. Since we use gridded tomography, the derivatives of migrated depths with respect to the model parameters are calculated at the vertices of relatively fine grids. Therefore, we follow Wang and Tsvankin (2010) in employing a mapping matrix to convert the model updates into the parameter values at each grid point. After 10 iterations, the CIGs are flat (Figures 6(a) and 6(b)) and the reflectors are tied in depth (Figures 7(a) and 7(b)). The estimated parameters of the VTI layer are close to the actual values: $V_{S0} = 1494$ m/s, $\epsilon = 0.1$, and $\delta = -0.09$.

Next, the algorithm is tested on a model (Figure 8) that includes a reflector (e.g., a fault plane) dipping at an angle approaching 30°. To avoid instability in ray tracing, we smooth the corner of the dipping interface using bicubic spline interpolation. The synthetic data include PP and PS reflections from both horizontal and dipping reflectors (Figure 9). The maximum offsets are 4 km for PP data and 2 km for SS-waves constructed by the PP+PS=SS method. Tsvankin and Grechka (2000) demonstrate that the traveltimes of the PP- and PS-waves reflected from a horizontal and a dipping interface are sufficient to constrain the parameters V_{P0}, V_{S0}, ϵ, and δ.

Here we only invert for the parameters of the middle layer. The initial model is isotropic with the velocities V_{P0} and V_{S0} distorted by 15%. The depth sections and CIGs computed with the initial model are displayed in Figures 10 and 11. A set of CIGs of PP- and SS-waves from both the horizontal and

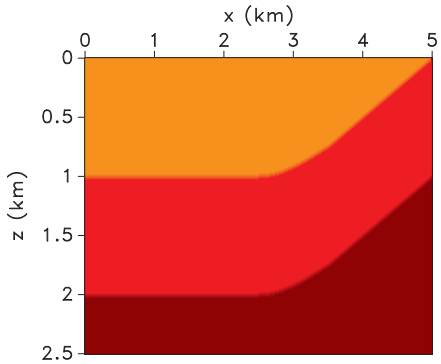

Figure 8. Three-layer VTI model with dipping interfaces. The parameters of the first layer are $V_P = 2000$ m/s, $V_S = 1000$ m/s; for the second layer, $V_{P0} = 3000$ m/s, $V_{S0} = 1500$ m/s, $\epsilon = 0.2$ and $\delta = 0.1$. The maximum dip of both reflectors is 27°.

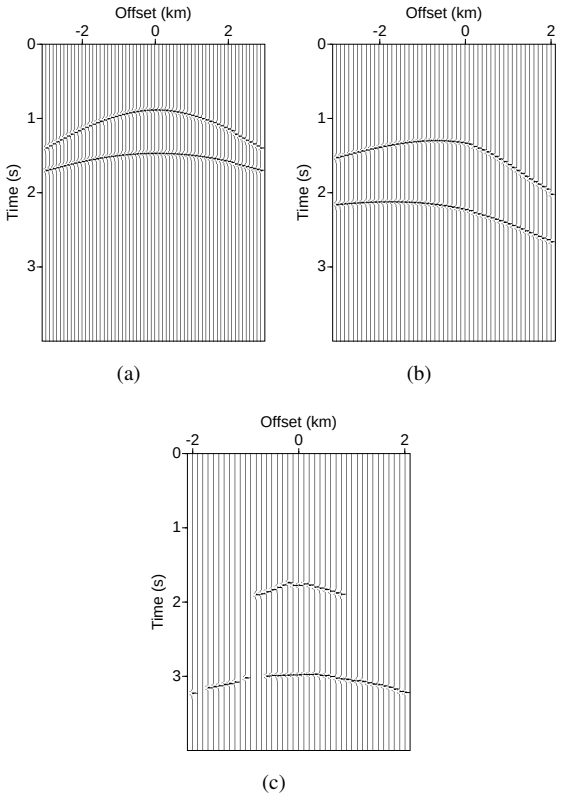

Figure 9. CMP gathers of the recorded (a) PP-waves and (b) PS-waves at location 3000 m. (c) The SS data constructed by the PP+PS=SS method at the same location.

dipping interfaces (for locations from 1 to 4 km) are used in the joint MVA. After 11 iterations, the image gathers are flat (Figures 12(a) and 12(b)) and the reflectors on the PP and SS sections are correctly positioned (Figures 13(a) and 13(b)). These results confirm the feasibility of building the VTI depth model using 2D PP and PS reflection data if both horizontal and dipping events are available. The inversion also produced accurate estimates of the interval VTI parameters: $V_{P0} = 3031$ m/s, $V_{S0} = 1515$ m/s, $\epsilon = 0.20$, and $\delta = 0.08$.

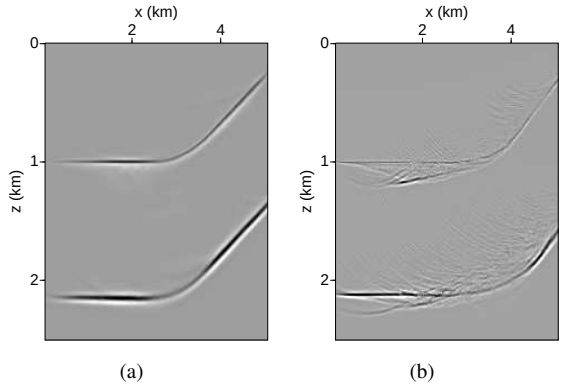

Figure 10. (a) PP-wave and (b) SS-wave depth images computed with the initial model parameters.

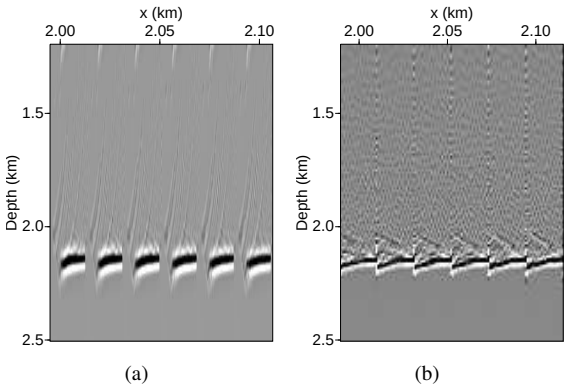

Figure 11. Common-image gathers of (a) PP-waves and (b) SS-waves (displayed every 100m) after migration with the initial model.

4 DISCUSSION AND CONCLUSIONS

In the presence of moderate dips, combining PP reflection traveltimes with converted PS data may help reconstruct VTI velocity models in depth. Here, we presented an efficient algorithm for joint migration velocity analysis of PP- and PS-waves from heterogeneous VTI media.

To avoid problems caused by the moveout asymmetry and other inherent features of mode conversions, we construct pure SS reflections using the PP+PS=SS method. Then migration velocity analysis is performed for PP and SS data, which allows us to employ existing tomographic techniques designed for pure modes. In addition to flattening common-image gathers of PP- and SS-waves, the joint MVA is designed to remove the depth misties between PP and SS sections. After performing prestack Kirchhoff depth migration on PP and SS data, we use a nonhyperbolic semblance scan to evaluate the long-spread residual moveout in CIGs. Then the velocity model is

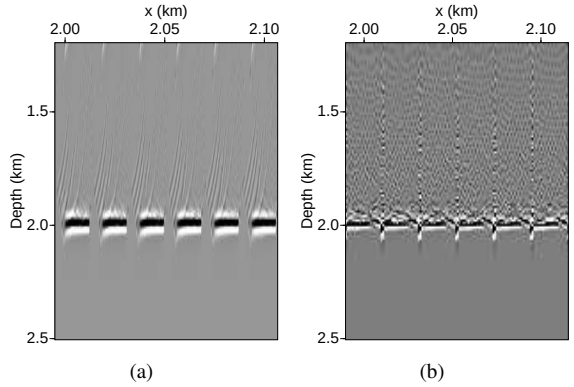

Figure 12. CIGs of (a) PP-waves and (b) SS-waves after migration with the inverted model.

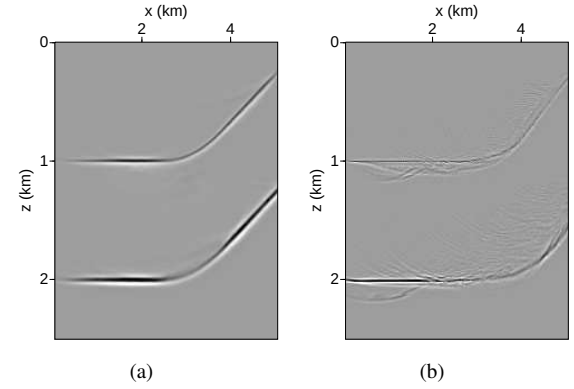

Figure 13. Final depth images of (a) PP-waves and (b) SS-waves obtained with the inverted model parameters.

updated iteratively by flattening PP- and SS-wave CIGs and tying of the PP and SS migrated images in depth.

Synthetic testing confirmed that if both horizontal and moderately dipping PP and PS events are available, the joint MVA converges toward the correct VTI depth model. Therefore, PS-waves can play an important role in velocity model building for prestack depth migration. Multicomponent data also provide accurate estimates of shear-wave vertical velocity V_{S0}, which can be used in lithology prediction and reservoir characterization.

5 ACKNOWLEDGMENTS

We are grateful to James Gaiser (Geokinetics) for helpful discussions and to the members of the A(nisotropy)-Team of the Center for Wave Phenomena (CWP) for valuable technical assistance.

APPENDIX A: PARAMETER UPDATING METHODOLOGY

We extend the MVA algorithm of Wang and Tsvankin (2010) to the combination of PP and SS data, where the SS-waves are constructed by the PP+PS=SS method. In addition to flattening PP and SS image gathers, we also perform codepthing to ensure that the reflectors on the PP and SS sections are imaged at the same depth. Following Wang and Tsvankin (2010), the variance Var of the migrated depths can be written as

$$Var = \sum_{j=1}^{U}\sum_{k=1}^{M}[z(x_j,h_k) - \hat{z}(x_j)]^2, \qquad \text{(A1)}$$

where U is the number of image gathers used in the velocity update, M is the number of offsets in image gathers, x_j is the midpoint, h_k is the half-offset, and $\hat{z}(x_j) = (1/M)\sum_{k=1}^{M} z(x_j,h_k)$ is the average migrated depth at x_j. By minimizing the variances Var_P (for P-waves) and Var_S (for S-waves), we flatten CIGs for both modes. The difference between the migrated depths of PP- and SS-waves from the same reflector can be estimated as:

$$Var_{P-S} = \sum_{j=1}^{U}[\hat{z_p}(x_j) - \hat{z_s}(x_j)]^2. \qquad \text{(A2)}$$

Minimizing Var_{P-S} makes it possible to tie the PP and SS sections in depth. Differentiating the variances with respect to the parameter updates $\mathbf{\Delta}\lambda$ and setting $\partial V/\partial(\mathbf{\Delta}\lambda) = 0$ yields

$$\mathbf{A}_P^T\mathbf{A}_P\mathbf{\Delta}\lambda = -\mathbf{A}_P^T\mathbf{b}_P \qquad \text{(A3)}$$

$$\mathbf{A}_S^T\mathbf{A}_S\mathbf{\Delta}\lambda = -\mathbf{A}_S^T\mathbf{b}_S \qquad \text{(A4)}$$

$$\mathbf{D}^T\mathbf{D}\mathbf{\Delta}\lambda = -\mathbf{D}^T\mathbf{y}, \qquad \text{(A5)}$$

where $\mathbf{A}$ is a $M*U$ by $W*N$ matrix with elements $g_{jk,ic} - \hat{g}_{j,ic}$, where $g_{jk,ic} = \partial z(x_j,h_k)/\partial\lambda_{ic}$ and $\hat{g}_{j,ic} = (1/M)\sum_{k=1}^{M} g_{jk,ic}$. The subscripts P and S denote P- and S-waves, respectively. The vector $\mathbf{b}$ contains $M*U$ elements defined as $z(x_j,h_k) - \hat{z}(x_j)$. $\mathbf{D}$ is also a $M*U$ by $W*N$ matrix and its elements are $g^P_{jk,ic} - g^S_{jk,ic}$, where $g^P_{jk,ic}$ is computed for P-waves and $g^S_{jk,ic}$ for S-waves. The $M*U$ vector $\mathbf{y}$ has elements $z^P(x_j,h_k) - z^S(x_j,h_k)$.As discussed in Wang and Tsvankin (2010), the derivatives $g_{jk,ic}$ are found by differentiating phase velocity with respect to the medium parameters along the raypath.

REFERENCES

Adler, F., R. Baina, M. A. Soudani, P. Cardon, and J.-B. Richard, 2008, Nonlinear 3d tomographic least-squares inversion of residual moveout in kirchhoff prestack-depth-migration common-image gathers: Geophysics, **73**, VE13–VE23.

Audebert, F., P. Y. Granger, and A. Herrenschmidt, 1999, CCP-Scan technique (*1): true common conversion point sorting and converted wave velocity analysis solved by PP and PS Pre-Stack Depth Migration: SEG Expanded Abstract, **18**, 1186–1189.

Bakulin, A., M. Woodward, D. Nichols, K. Osypov, and O. Zdraveva, 2010, Building tilted transversely isotropic depth models using localized anisotropic tomography with well information: Geophysics, **75**, D27–D36.

Broto, K., A. Ehinger, J. H. Kommedal, and P. G. Folstad, 2003, Anisotropic traveltime tomography for depth consistent imaging of PP and PS data: The Leading Edge, 114–119.

Du, Q., F. Li, J. Ba, Y. Zhu, and B. Hou, 2012, Multicomponent joint migration velocity analysis in the angle domain for PP-waves and PS-waves: Geophysics, **77**, U1–U13.

Foss, S., B. Ursin, and M. V. de Hoop, 2005, Depth-consistent reflection tomography using PP and PS seismic data: Geophysics, **70**, U51–U65.

Grechka, V., A. Pech, and I. Tsvankin, 2002a, Multicomponent stacking-velocity tomography for transversely isotropic media: Geophysics, **67**, 1564–1574.

Grechka, V., and I. Tsvankin, 2002, PP+PS=SS: Geophysics, **67**, 1961–1971.

Grechka, V., I. Tsvankin, A. Bakulin, J. O. Hansen, and C. Signer, 2002b, Joint inversion of pp and ps reflection data for VTI media: A north sea case study: Geophysics, **67**, 1382–1395.

Sarkar, D., and I. Tsvankin, 2004, Migration velocity analysis in factorized VTI media: Geophysics, **69**, 708–718.

Stopin, A., and A. Ehinger, 2001, Joint PP PS tomographic inversion of the mahogany 2D 4-C OBC seismic data: SEG Expanded Abstract, 837–840.

Stork, C., 1992, Reflection tomography in the postmigrated domain: Geophysics, **57**, 680–692.

Thomsen, L., 1999, Converted-wave reflection seismology over inhomogeneous, anisotropic media: Geophysics, **64**, 678–690.

Tsvankin, I., 2005, Seismic signatures and analysis of reflection data in anisotropic media, 2nd: Elsevier Science Publishing Company, Inc.

Tsvankin, I., and V. Grechka, 2000, Dip moveout of converted waves and parameter estimation in transversely isotropic media: Geophysical Prospecting, **48**, 257–292.

———, 2011, Seismology of azimuthally anisotropic media and seismic fracture characterization: Society of Exploration Geophysicists.

Tsvankin, I., and L. Thomsen, 1995, Inversion of reflection traveltimes for transverse isotropy: Geohpysics, **60**, 1095–1107.

Wang, B., K. Pann, and R. A. Meek, 1995, Macro velocity model estimation through model based globally-optimized residual-curvature analysis: SEG Expanded Abstract, 1084–1087.

Wang, X., and I. Tsvankin, 2010, Ray-based gridded tomography for tilted TI media: CWP Project Review Report, 95–108.

Zhou, C., J. Jiao, S. Lin, J. Sherwood, and S. Brandsberg-Dahl, 2011, Multiparameter joint tomography for TTI model building: Geophysics, **76**, WB183–WB190.